Superconducting Properties of $NdO_{0.5}F_{0.5}BiS_2$ Single Crystals

Qian Chen, Mahmoud Abdel-Hafiez, Xiao-Jia Chen, Zhixuan Shen, Yihao Wang, Chunmu Feng & Zhu'an Xu

Journal of Superconductivity and Novel Magnetism
Incorporating Novel Magnetism

ISSN 1557-1939

J Supercond Nov Magn
DOI 10.1007/s10948-016-3436-z

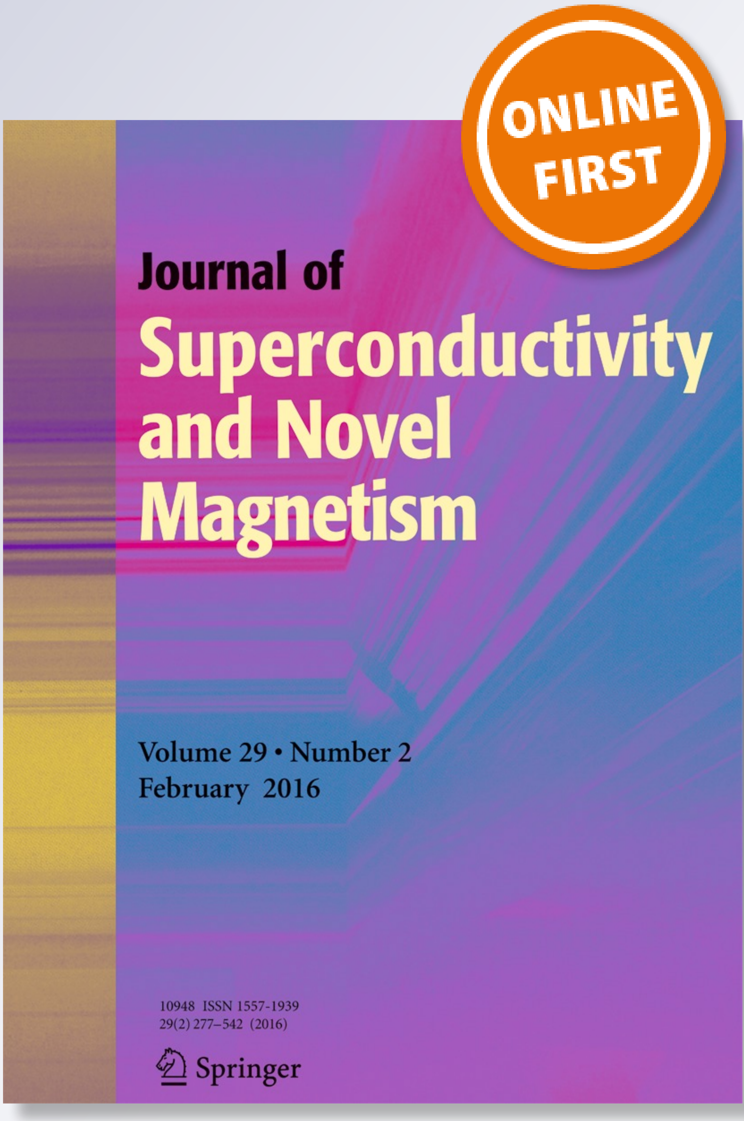

Springer

J Supercond Nov Magn
DOI 10.1007/s10948-016-3436-z

ORIGINAL PAPER

HPSTAR 2016-269

Superconducting Properties of $NdO_{0.5}F_{0.5}BiS_2$ Single Crystals

Qian Chen[1] · Mahmoud Abdel-Hafiez[2] · Xiao-Jia Chen[2] · Zhixuan Shen[1] · Yihao Wang[1] · Chunmu Feng[1] · Zhu'an Xu[1,3]

Received: 21 January 2016 / Accepted: 23 January 2016

Abstract We report on superconducting properties of high-quality single crystals of F-substituted $NdOBiS_2$ using low-temperature magnetization and transport measurements. Using the mixture of CsCl and KCl as the flux, we have synthesized our single crystals. This compound exhibits bulk superconductivity with a transition temperature of about $T_c \sim 4.6$ K. The critical current density J_c as a function of temperature has been derived and decreases with the increasing temperature. We construct the phase diagram $H_{c2}(T)$. The zero-temperature value for $H_{c2}^{B\|c}$ for value for $T_c^{90\ \%}$ and $T_c^{0\ \%}$ is estimated to be approximately 2.17 and 1.72 T respectively by using Werthamer-Helfand-Hohenberg model.

Keywords BiS_2-based superconductors · Electrical transport · Magnetization · Pairing symmetry

✉ Mahmoud Abdel-Hafiez
m.mohamed@hpstar.ac.cn

1 Department of Physics and State Key Laboratory of Silicon Materials, Zhejiang University, Hangzhou 310027, China

2 Center for High Pressure Science and Technology Advanced Research, Shanghai 201203, China

3 Zhejiang California International NanoSystems Institute, Zhejiang University, Hangzhou 310058, People's Republic of China

1 Introduction

The recent discovery of superconductivity (SC) in BiS_2-based superconductors $Bi_4O_4S_3$ [1, 2] and $LnO_{1-x}F_xBiS_2$ (Ln = La, Ce, Pr, Nd, and Yb) [3–6], has generated enormous interest in condensed-matter physics. The superconductors $LnO_{1-x}F_xBiS_2$ have a layered crystal structure of stacked BiS_2 superconducting and $LnO_{1-x}F_x$ block layers, which resembles the structures of cuprate and iron pnictide superconductors. The critical transition temperature (T_c) of $LnO_{0.5}F_{0.5}BiS_2$ (Ln = rare earth) whose parent phase exhibits a semiconductor-like behavior [7] increases abruptly from 2.5 K to above 10 K at a small pressure of 0.7 GPa [8, 9]. Similar results in $Sr_{0.5}RE_{0.5}BiS_2$ (RE = Ce, Nd, Pr, and Sm) [10] and $Eu_3Bi_2S_4F_4$ [11] compounds were also observed. A first-principles calculation shows that BiS_2-based compounds are strong electron-phonon coupled superconductors in the vicinity of competing ferroelectric and charge-density wave (CDW) phases [12]. A CDW-like transition has indeed been observed in both $EuBiS_2F$ [13] and $Eu_3Bi_2S_4F_4$ [14].

The BiS_2-based system possesses many attractive features and there is controversy about the nature of pairing from both theoretical and experimental sides. Triplet pairing and and g-wave pairing in these superconductors were theoretically proposed by Yang et al. [15] and Wu et al. [16] respectively, suggesting that the pairing mechanism could be unconventional. Recently, a theoretical calculation has proposed that extended *s*-wave symmetry always wins over *d*-wave assuming that the moderate electron-electron correlation is important [17]. Meanwhile, a mixture

Published online: 03 February 2016

of both symmetries (B_{2g} and A_{1g}) was predicted based on random-phase approximation analysis of a two-orbital model [18]. Experimentally, the observation of nodeless SC in these compounds using the tunnel-diode-oscillator technique have been reported recently [19, 22], providing evidences of *s*-wave character of the order parameter. However, an unexpected giant superconducting fluctuation appears in $NdO_{1-x}F_xBiS_2$ and two gap features were observed by scanning tunneling spectroscopy [23]. At present, there is no consensus on the pairing symmetry in BiS_2-based compounds which requires further theoretical and experimental studies.

One of the central points in this paper is to reliably determine the superconducting properties of the optimal doped single crystals $NdO_{0.5}F_{0.5}BiS_2$ from low-temperature transport and magnetization measurements. The lower critical field H_{c1} and the critical current density J_c have been determined from detailed measurements of magnetic property. The upper critical field $H_{c2}^{90\,\%}(0)$, $H_{c2}^{50\,\%}(0)$, and $H_{c2}^{0\,\%}(0)$ as a function of temperature were obtained using the criteria of 90 %ρ_n, 50 %ρ_n, and 0 %ρ_n (ρ_n is the normal state resistivity), respectively. We propose that linear H_{c1} and H_{c2} versus T data can be well described by the single band *s*-wave pairing model.

2 Method

Single crystals of $NdO_{0.5}F_{0.5}BiS_2$ were grown using the mixture of CsCl and KCl as the flux, similar to the previous reports [24]. All the preparation procedures except the heating were carried out in an argon-filled glove box where the water and oxygen contents are less than 0.1 ppm. As a first step, Nd_2S_3 was presynthesized by reacting Nd and S powders in vacuum at 673 K for 10 h and then at 1173 K for 12 h. The accurately weighed stoichiometric mixture of Nd_2S_3, Bi, Bi_2S_3, Bi_2O_3, BiF_3, CsCl, and KCl were thoroughly mixed using a agate mortar. The mixture was loaded in a quartz tube. The sealed quartz ampoule was heated to 1103 K, holding at this temperature for 10 h. Then, it was slowly cooled to 883 K at a rate of 2 K/h. The obtained samples were washed with distilled water.

Powder x-ray diffraction (XRD) was carried out at room temperature using a PANalytical X-ray diffractometer with $CuK_{\alpha 1}$ radiation. Electrical resistivity was measured by a standard four-terminal method. We contacted the single crystals with fine gold wires then fixed them with silver adhesive. Transport properties were performed on a Quantum Design physical property measurement system (PPMS). Magnetization measurements were carried out on a Quantum Design magnetic property measurement system (MPMS).

3 Results and Discussions

Figure 1 shows the XRD pattern for the $NdO_{0.5}F_{0.5}BiS_2$ single crystal at room temperature. Only (0 0 l) peaks were observed and the full width at half maximum (FWHM) was found to be 0.1° indicating a well developed *ab*-plane orientation of these single crystals. The peak positions agree very well with data from other groups described in the literatures [25]. The lower inset shows the dimension of the crystal and the direction of applied magnetic field. Shining single crystals shown in the upper inset with a typical size of $1\times0.8\times0.04\,(\pm0.02)\,mm^3$ were used in our measurements.

Figure 2 presents the magnetic data for single crystals of $NdO_{0.5}F_{0.5}BiS_2$ single crystals. Figure 2a, b shows the temperature dependence of the magnetization measured over the range from 1.8 to 300 K under an external magnetic field of 1 kOe along the *ab*-plane and *c*-axis, respectively. The *M(T)* are linear at high temperatures and a Curie-like upturn is observed below 100 K showing a typical paramagnetic behavior. The insets of Fig. 2a, b show the temperature dependence of the magnetic susceptibility ($\chi = M/H$) measured by following zero-field cooled (ZFC) procedures in an external field of 10 Oe applied along *c* axis. The DC magnetic susceptibility exhibits a superconducting temperature transition with an onset at 4.6 K of both orientations. We should mention that the very small thickness of the single sheets have a significant influence on the accuracy of magnetic shielding fraction. The magnetic shielding fraction of the sample was estimated to be 15 % at 2 K. From the insets of (b), we see that the in-plane magnetization is

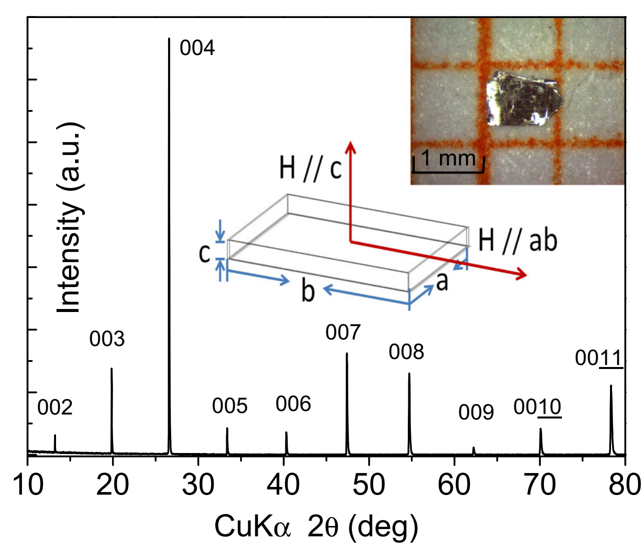

Fig. 1 X-ray diffraction pattern of $NdO_{0.5}F_{0.5}BiS_2$ single crystal. *Upper inset*: a typical photo of $NdO_{0.5}F_{0.5}BiS_2$ crystal. *Lower inset*: the orientation of the crystal in the experiments

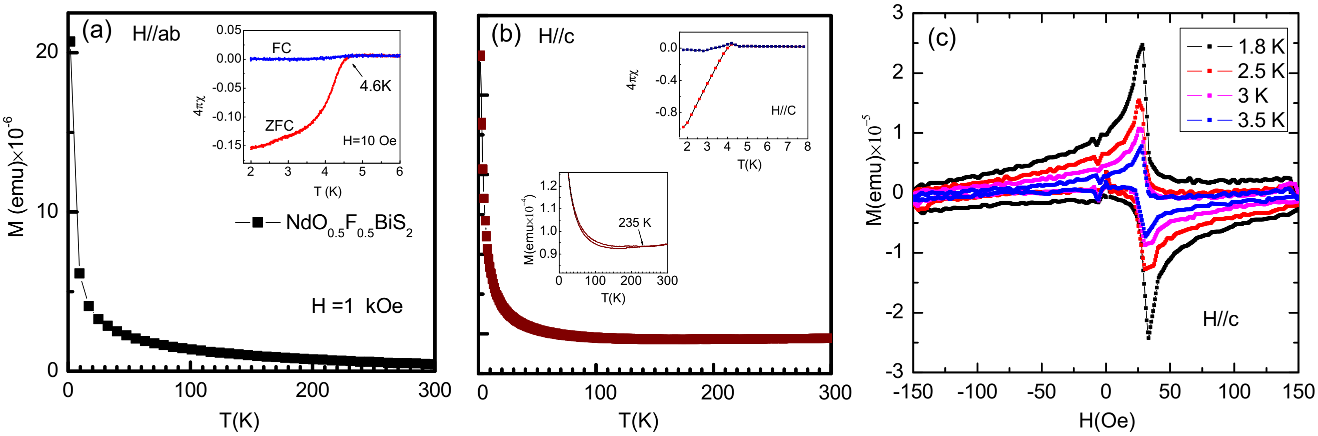

Fig. 2 The magnetic measurements for $NdO_{0.5}F_{0.5}BiS_2$ single crystals. **a**, **b** Temperature dependence of the magnetization measured under a magnetic field of 1000 Oe along ab plane and c axis, respectively. Insets of (**a**, **b**) show magnetic susceptibility χ(T) data. Field-cooling protocols were used under the field of 10 Oe along ab plane and c axis, respectively. **c** It the magnetic hysteresis loops after subtracting a paramagnetic background. These MHLs were measured at various temperatures T = 1.8, 2.5, 3, 3.5, and 8 K

around 30 %, two times as large as the $H \parallel ab$ case which may be due to the diamagnetic factor. Figure 2c displays the magnetic hysteresis loops (MHLs). These loops have been measured at various temperatures (T = 1.8, 2.5, 3, and 3.5 K) after subtracting a paramagnetic background measured at 8 K, while the external magnetic field is always along the c axis. The shape of MHLs and the hysteresis reflect a type-II superconductor characteristic.

From the magnetization hysteresis loops $M(H)$, we calculated the critical current density J_c by using the critical state model with the assumption of field-independent J_c. By definition, J_c is given by [26]:

$$J_c = \frac{20\Delta M}{a\left(1 - \frac{a}{3b}\right)}, \tag{1}$$

Where $\Delta M = M_{down}$-M_{up}, M_{down}, and M_{up} refer to the magnetization values in the process of decrease and increase of magnetic field, respectively, and a and b are the sizes of the platelet samples ($a < b$, shown in Fig. 1). Figure 3 shows the critical current J_c as a function of magnetic field of one sample with the sizes of $a = 0.7999$ mm and $b = 0.9066$ mm. In this case, J_c at 1.8 K was found to be 1.045×10^4 A/cm^2 for $H \parallel c$. Meanwhile, in the inset of (b), we displayed the critical current density at different temperatures without external field. On account of the irregular jumps close to $H = 0$, the error bars were added. The uncertainty of the current density is

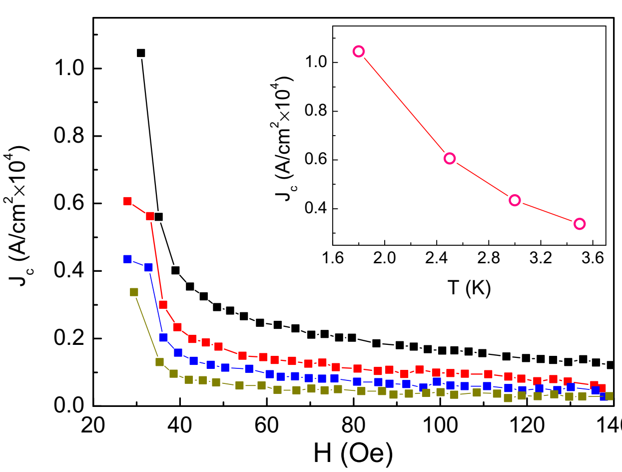

Fig. 3 The critical current J_c as a function of magnetic field. Inset: temperature dependence of the critical current without magnetic field

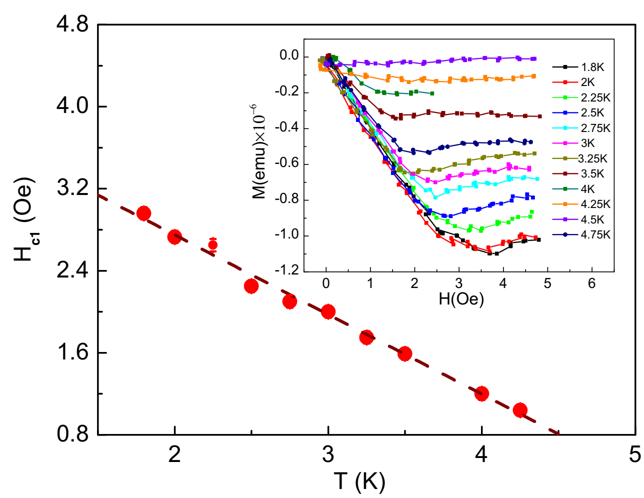

Fig. 4 The lower critical field of $NdO_{0.5}F_{0.5}BiS_2$ single crystals for the field applied along the c axis. The *red brown dot line* is a linear fit of the data. The inset shows the field dependence of initial part of magnetization curves, measured at various temperatures for $H \parallel$ c

Fig. 5 **a** Temperature dependence of the electrical resistivity ρ measured in the ab plane of $NdO_{0.5}F_{0.5}BiS_2$. The inset shows definition of the characteristic temperature $T_c{}^{90\,\%}$, $T_c{}^{50\,\%}$, and $T_c{}^{0\,\%}$ of the superconducting transition. **b** Magnetoresistivity for magnetic fields H parallel to the c axis ($H = 0 \sim 1$ T)

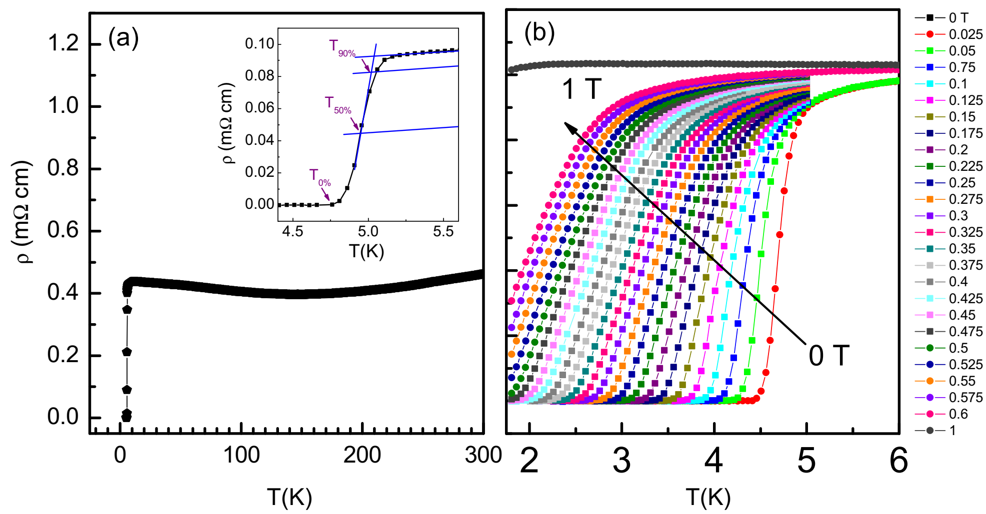

200 A/cm^2. As we can see, J_c decreased with the increasing temperature.

The fact that the hysteresis loops for both orientations are symmetric around $M = 0$, points to the relatively weak surface barriers and is indicative of a strong bulk pinning [21]. This consideration holds for all studied temperatures, even close to T_c and guarantees that vortex penetration occurs at a field close to H_{c1}. In contrast to that, if surface barriers were predominant, the first vortex entrance can occur a much higher field ($\sim H_c$). It is worth noting that the superconducting $M(H)$ exhibits a very weak magnetic background. This indicates that the sample contains negligible magnetic impurities. The virgin $M(H)$ curves at low fields at several temperatures are collected in Fig. 4 for $H \parallel c$. In order to determine the transition from linear to non-linear $M(H)$, a user-independent procedure consisting of calculating the regression coefficient R of a linear fit to the data points collected between 0 and H, as a function of H is used. Then, H_{c1} is taken as the point where the function $R(H)$ starts to deviate from linear dependence. This procedure is similar to that previously used in the studies shown in the ref. [20]. These $M - H$ curves are linear at low H, then deviate from linearity at higher fields indicating the first vortex penetration. We obtained the phase diagram of H_{c1} from these curves which exhibited a linear behavior obviously (see Fig. 4). The red brown dot line is a guide for the eyes. This phenomenon is consistent with the full-gap s-wave pairing symmetry. The lower critical $H_{c1}(0)$ was identified as 4.3 Oe.

Figure 5a shows the temperature dependence of the electrical resistivity ρ measured in the ab plane of $NdO_{0.5}F_{0.5}BiS_2$. Metallic behavior is observed above 140 K then a pronounced upturn shows up when temperature decreases. Upon lowering T, the resistivity displays a drop to zero as shown in the inset of Fig. 5a. We defined the characteristic temperature $T_c{}^{90\,\%}$, $T_c{}^{50\,\%}$, and $T_c{}^{0\,\%}$ of the superconducting transition where $\rho(T)$ drops to 90, 50, and 0 % of the normal state value, respectively, as illustrated in the inset of Fig. 5a. Here, the $T_c^{90\,\%}$, $T_c^{50\,\%}$, and $T_c^{10\,\%}$ criteria of the normal state have been used to extract the T_c at each magnetic field, see the inset of Fig. 5a. The zero-field resistivity shows an onset transition at 5.07 K and zero resistance was observed at 4.76 K. These values are inline with the magnetic susceptibility χ(T) measurement. The suppression of superconductivity is clearly obvious upon applying magnetic field, indicating the nature of superconductivity in our systems. At low temperatures, the curves are almost parallel with respect to each other in the transition region. With increasing magnetic

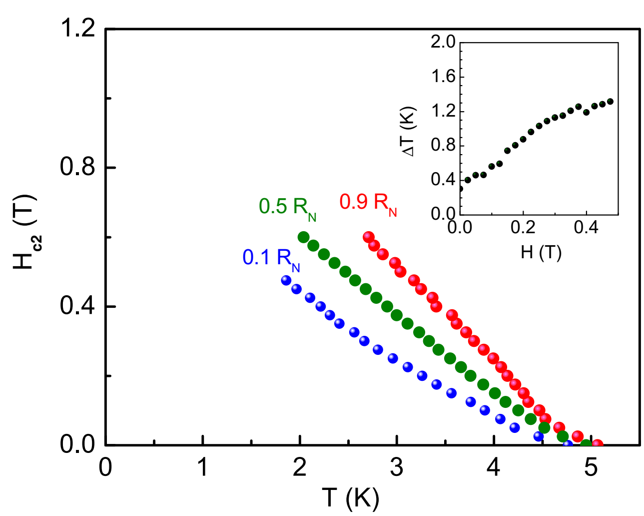

Fig. 6 The upper critical fields H_{c2} ($H_{c2}^{90\,\%}$, $H_{c2}^{50\,\%}$, and $H_{c2}^{0\,\%}$) as a function of temperature for $NdO_{0.5}F_{0.5}BiS_2$ single crystals. The inset shows temperature difference between $H_{c90\,\%}$ and $H_{c0\,\%}$

fields, the onset of superconductivity shifts to lower temperatures gradually. The superconducting transition width is only 0.3 K indicating a high quality of our samples. However, the inset of Fig. 6b displays the field dependence of the width of the transitions shown in Fig. 5b. The width is determined by the difference between the $T_c^{90\,\%}$ and the zero resistivity value of T_c. The difference becomes more and more significant with increasing external magnetic field

Exploring the field dependance and the upper critical field in the of $NdO_{0.5}F_{0.5}BiS_2$ are very important factors which help reveal the mechanism of the nature of the superconductivity of this system. We plotted the upper critical fields H_{c2} as a function of temperature in Fig. 6. The $H_{c2}^{90\,\%}$, $H_{c2}^{50\,\%}$, and $H_{c2}^{0\,\%}$ data extracted from magnetorisistivity measurement exhibit a linear temperature dependence with average slopes of -$(dH_{c2}^{90\,\%}/dT)_{T_c}$ = 2.81 T/K, -$(dH_{c2}^{90\,\%}/dT)_{T_c}$ = 2.17 T/K and -$(dH_{c2}^{0\,\%}/dT)_{T_c}$ = 1.72 T/K, respectively. We estimated $H_{c2}^{90\,\%}(0)$, $H_{c2}^{50\,\%}$ and $H_{c2}^{0\,\%}(0)$ using the single-band Wethamer-Helfand-Hohenberg (WHH) model $H_{c2}(0) = -0.69T_c(dH_{c2}/dT)_{T_c}$. The values were found to be 9.824 T, 7.412 T, and 5.653 T, respectively. The upper critical fields (determined using the different criteria mentioned above) all exhibit a linear behavior consistent with each other, which is expected for a fully gapped s-wave superconductor.

4 Summary

In summary, the superconducting properties of F-substituted $NdOBiS_2$ single crystals were studied by performing detailed megnetization and resistivity measurements. The superconducting transition temperature T_c (4.76 K), critical magnetic field H_{c1} (4.3 Oe), $H_{c2}^{90\,\%}$ (9.824 T), $H_{c2}^{50\,\%}$ (7.412 T), and $H_{c2}^{0\,\%}(0)$ (5.653 T) were extracted from the experimental data. Temperature and field dependence of the critical current density J_c have been determined from magnetic measurements. Linear temperature dependence of both H_{c1} and H_{c2} was found, which provides an evidence for a single band s-wave paring symmetry.

Acknowledgments This work was supported by the National Basic Research Program of China (Grant Nos. 2014CB921203, and 2012CB927404), NSF of China (Contract Nos. U1332209 and 11190023), and the Fundamental Research Funds for the Central Universities of China.

References

1. Mizuguchi, Y., Fujihisa, H., Gotoh, Y., Suzuki, K., Usui, H., Kuroki, K., Demura, S., Takano, Y., Izawa, H., Miura, O.: Phys. Rev. B **86**, 220510 (2012)
2. Singh, S.K., Kumar, A., Gahtori, B., Sharma, G., Patnaik, S., Awana, V.P.S.: J. Am. Chem. Soc. **134**, 16504 (2012)
3. Mizuguchi, Y., Demura, S., Deguchi, K., Takano, Y., Fujihisa, H., Gotoh, Y., Izawa, H., Miura, O.: J. Phys. Soc. Jpn. **81**, 114725 (2012)
4. Xing, J., Li, S., Ding, X., Yang, H., Wen, H.-H.: Phys. Rev. B **86**, 214518 (2012)
5. Demura, S., Mizuguchi, Y., Deguchi, K., Okazaki, H., Hara, H., Watanabe, T., James Denholme, S., Fujioka, M., Ozaki, T., Fujihisa, H., Gotoh, Y., Miura, O., Yamaguchi, T., Takeya, H., Takano, Y.: J. Phys. Soc. Jpn. **82**, 033708 (2013)
6. Yazici, D., Huang, K., White, B.D., Chang, A.H., Friedman, A.J., Maple, M.B.: Phil. Mag. **93**, 673 (2013)
7. Awana, V.P.S., Kumar, A., Jha, R., Singh, S.K., Pal, A., Shruti, K., Saha, J., Patnaik, S.: Solid State Commun. **157**, 21 (2013)
8. Tomita, T., Ebata, M., Soeda, H., Takahashi, H., Fujihisa, H., Gotoh, Y., Mizuguchi, Y., Izawa, H., Miura, O., Demura, S., Deguchi, K., Takano, Y.: J. Phys. Soc. Jpn. **83**, 063704 (2014)
9. Wolowiec, C.T., Yazici, D., White, B.D., Huang, K., Maple, M.B.: Phys. Rev. B **88**, 064503 (2013)
10. Jha, R., Tiwari, B., Awana, V.P.S.: J. Appl. Phys. **117**, 013901 (2015)
11. Luo, Y., Zhai, H.-F., Zhang, P., Xu, Z.-A., Cao, G.-H., Thompson, J.D.: Phys. Rev. B **90**, 220510 (2014)
12. Yildirim, T.: Phys. Rev. B **87**, 020506 (2013)
13. Zhai, H.-F., et al.: Phys. Rev. B **90**, 064518 (2014)
14. Zhang, P., Zhai, H.-F., Cao, G., Xu, Z.: Bull. Am. Phys. Soc. **60** (2015)
15. Yang, Y., Wang, W., Xiang, Y., Li, Z., Wang, Q.: Phys. Rev. B **88**, 94519 (2013)
16. Wu, X.X., Yuan, J., Liang, Y., Fan, H., Hu, J.P.: Euro- Phys. Lett. **108**, 027006 (2014)
17. Liang, Y., Wu, X., Tsai, W.-F., Hu, J.: Front. Phys. **9**, 194–199 (2014)
18. Martins, G.B., Moreo, A., Dagotto, E.: Phys. Rev. B **87**, 081102 (2013)
19. Shruti, K., Srivastava, P., Patnaik, S.: J. Phys.:Condens. Matter. **25**, 312202 (2013)
20. Abdel-Hafiez, M., Ge, J., Vasiliev, A.N., Chareev, D.A., Van de Vondel, J., Moshchalkov, V.V., Silhanek, A.V.: Phys. Rev. B **88**, 174512 (2013)
21. Abdel-Hafiez, M., et al.: Phys. Rev. B **90**, 054524 (2014)
22. Jiao, L., Weng, Z., Liu, J., Zhang, J., Pang, G., Guo, C., Gao, F., Zhu, X., Wen, H.-H., Yuan, H.Q.: J. Phys.:Condens. Matter **27**, 225701 (2015)
23. Liu, J., Fang, D., Wang, Z., Xing, J., Du, Z., Zhu, X., Yang, H., Wen, H.-H.: Europhys. Lett. **106**, 67002 (2014)
24. Masanori, N., et al.: Solid State Commun. **178**, 33–36 (2014)
25. Nagao, M., et al.: J. Phys. Soc. Jpn. **82**, 113701 (2013)
26. Bean, C.P.: Phys. Rev. Lett. **8**, 250–253 (1962)